

Far-infrared absorption by aluminum small particles

Y. H. Kim* and D. B. Tanner

Department of Physics, University of Florida, Gainesville, Florida 32611

(Received 10 March 1988; revised manuscript received 2 November 1988)

The far-infrared (FIR) absorption of small particles has been studied for a variety of sizes of aluminum small particles. The particle size dependence of the FIR absorption coefficient was obtained. In addition, the FIR absorption coefficients of clustered samples and nonclustered random samples were measured. The small-particle composite samples were characterized with scanning-transmission electron microscope analyses. Our data suggest that individual small particles are responsible for the anomalous FIR absorption. Also, we found a particle size dependence of the FIR absorption coefficient which differs from the predictions made by classical theory. These discrepancies imply that the Drude model may not be an adequate description of FIR dielectric function of small metal particles.

I. INTRODUCTION

The anomalous far-infrared (FIR) absorption by small metal particles¹⁻⁸ has been a puzzling problem for more than a decade. Although classical theories (such as Mie theory and Maxwell-Garnett theory) give a correct description of the scattering and absorption of light by small particles in the visible frequency region,⁹ they predict far too small a FIR absorption.

Many theoretical models have been proposed to explain this peculiar FIR phenomenon in small particle systems, including quantum size effects,¹⁰⁻¹² direct coupling of external electric fields to phonons through the unscreened surface ions in the small particle,¹³ nonlocal effects,¹⁴ and absorption in poorly conducting oxide coatings.^{7,8,15,16} Recently, many workers¹⁶⁻²⁰ have demonstrated that calculated FIR absorption can be enhanced to be close to the experimental results if particles are clustered or clumped together. In this latter case the absorption is attributed to either large electric dipole absorption caused by poor effective dc conductivity of individual clusters of small particles or to the magnetic dipole absorption of fused clusters, which provide a large eddy current loop. Because there was no convincing direct experimental evidence of the randomness of the dispersed small particles in the insulating medium, the assumption of clustering of individual small particles was a plausible explanation of the FIR absorption.

In the experiments in question,¹⁻⁸ small particles typically are prepared by evaporation in an inert-gas atmosphere.⁴ A small amount of oxygen is normally introduced to guarantee electrical isolation between particles by forming a metal oxide layer on the surfaces of the particles. These small particles are dispersed in a FIR transparent insulating medium at a given volume fraction for transmission measurements. For small volume fraction, the measured FIR absorption coefficient has the approximately quadratic frequency dependence and the linear metal-particle volume-fraction dependence of theory for small volume fraction but is orders of magnitude larger

than theory. The only case where a nonlinear dependence on metal volume fraction was observed was the measurements of Carr *et al.*⁵ on aluminum particles embedded in KCl. Recently, Devaty and Sievers⁶ reported an experiment on a different small-particle system, order of 100-Å Ag particles embedded in a gelatin matrix, in which they were able to control the dispersion of the particles. They found that a clustered sample had a much larger FIR absorption coefficient than a well-dispersed sample. But there the nonclustered Ag particle sample still showed a factor of 100 times larger absorption than theory. In addition, Lee *et al.*⁷ and Noh *et al.*⁸ studied the FIR absorption for fairly large Ag particles (radius $a > 500$ Å) embedded in a Teflon matrix, finding that the FIR absorption of well-isolated Ag particles is close to the classical predictions if the contribution of the poorly conducting oxide coating is included.

In this paper, we describe measurements of the FIR absorption coefficient of aluminum small particles embedded in an insulating host, KCl. Very small volume fractions ($0.001 \leq f \leq 0.032$) were employed so that the samples were well below the critical concentration for percolation ($f_c \approx 0.18$). We systematically studied the particle size and concentration dependence of the FIR absorption. In addition, we investigated the effect of clustering on the FIR absorption coefficient by deliberately preparing clustered small-particle-KCl composites. Characterization of the small-particle composites was done using scanning transmission electron microscopy (STEM) for both clustered and nonclustered samples.

II. EXPERIMENT

Small particles were prepared by the gas-evaporation technique.²¹ Pure aluminum (about 200 mg) was evaporated under an inert-gas atmosphere. Helium or argon gas at pressure of 1-10 Torr was used, with the size of particles determined by the atomic mass and pressure of the inert gas used.

For the infrared measurements, aluminum small parti-

cles were mixed with an insulating dielectric medium (KCl in this work) to obtain the chosen metallic volume fraction. The volume fraction f was calculated from the weight of the two constituents, assuming bulk densities. In order to improve the homogeneity of the small-particle composite, the powder was mixed in a "freezer mill" operating at 77 K, compressed in an evacuated die into a $\frac{5}{8}$ -in.-diam pellet, reground, and recompressed. Before each compression, the ground Al-KCl powders were baked for several hours under vacuum at 150°C to reduce their moisture content. The compression took place at 130 000 psi (9 kbar) pressure, yielding a density ($f=0$ sample) equal to that of single crystalline KCl. This pressing-regrinding-pressing process was repeated four to six times.

A lamellar grating interferometer²² was used over frequencies between 2 and 60 cm^{-1} and a Michelson interferometer²³ covered frequencies between 10 and 100 cm^{-1} . Sample temperatures were 1.2 or 4.2 K; no temperature dependence was observed. The FIR absorption coefficient was calculated from measured transmittance, using the following formula:

$$\alpha_{\text{expt}} = -(1/d)\ln T + (2/d)\ln(1-R). \quad (1)$$

Here, α_{expt} is the absorption coefficient, d is the thickness of the sample (typically 0.5–5.0 mm), T is the measured transmittance, and R is the reflectance of the sample. Typically, the reflectance of a composite sample with $f < 0.03$ is close to that of pure KCl and essentially frequency independent in the frequency range of interest.²⁴ Therefore, the reflectance of pure KCl was used in the data analysis.

One remark about the FIR measurements of small-particle composites is that an interference pattern in the transmission spectrum, which is due to multiple internal reflections within the finite thickness of sample, is inevitable. These fringes occur at a frequency spacing of $\Delta\nu = (2nd)^{-1}$, where ν is the frequency in cm^{-1} , n is the refractive index, and d is the sample thickness. The interference pattern may be removed from the absorption spectrum by making measurements at reduced spectral resolution. A method applied in this work to eliminate the interference pattern is to make the effective thickness of the sample be large enough that the fringe spacing is much smaller than the resolution by adding an extra layer of KCl to the Al-KCl composite sample. So long as the difference between the refractive indices of the composite and pure KCl layer is negligible, this method works well.

In cases where the extra KCl layer was not used, information about the dielectric constant of the composites can be determined from the interference fringes. This analysis is most easily done by Fourier transforming the absorption coefficient, after removing the overall quadratic frequency dependence. The Fourier-transformed result shows a Lorentzian-shape power spectrum peaked at $x = 2nd$ because the amplitude of the interference fringes decays as the frequency increases due to absorption. The dielectric constant is then $\epsilon_1 = n^2$.

After the FIR measurements were finished, each sample was cut into a 3-mm-diam pellet, ground down to

100- μm thickness, and then dimpled until the thickness of the thinnest portion became about 10 μm . An ion mill or chemical polisher was then used to make a pinhole in the dimpled specimen. The STEM pictures were taken in the vicinity of the pinhole where electrons can be transmitted. About ten to fifteen different areas were examined for each sample.

III. RESULTS

Typical STEM results of well-dispersed small-particle composites are shown in Figs. 1(a) and 1(b) for two different samples. Figure 1(a) shows a sample with a relatively high volume fraction, $f=0.032$, whereas Fig. 1(b) shows one with a low volume fraction, $f=0.001$. In each case individual particles embedded in KCl matrix can be seen in the STEM pictures. (The particles are the black spots in the picture; the grey ripples are associated with the KCl.)

Figure 2 shows a direct comparison of the clustered samples prepared without using the freezer mill and non-clustered samples prepared by using the freezer mill. The nonclustered samples [Figs. 2(a) and 2(b)] were made after four pressing-regrinding-pressing cycles; only a single mixing compression was used for the clustered samples [Figs. 2(c) and 2(d)]. Note that individual particles

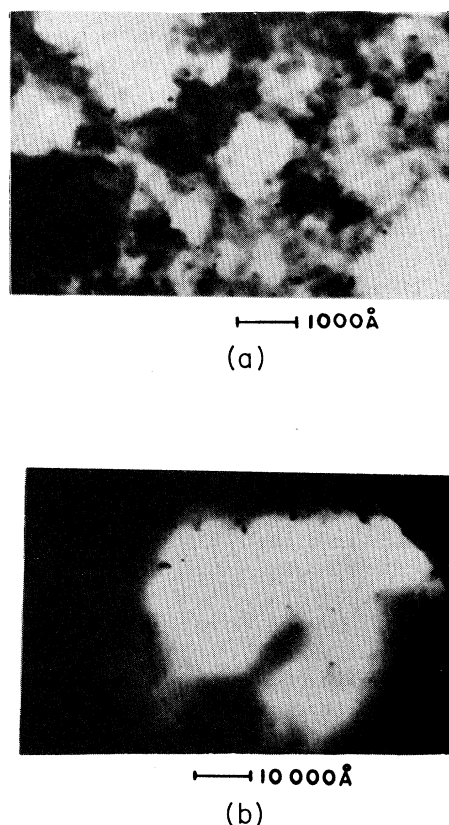


FIG. 1. Transmission electron micrographs of Al-KCl composites: (a) chemically polished $f=0.032$ Al ($a=85 \text{ \AA}$) sample (reground six times); (b) ion milled $f=0.001$ Al ($a=399 \text{ \AA}$) sample (reground four times).

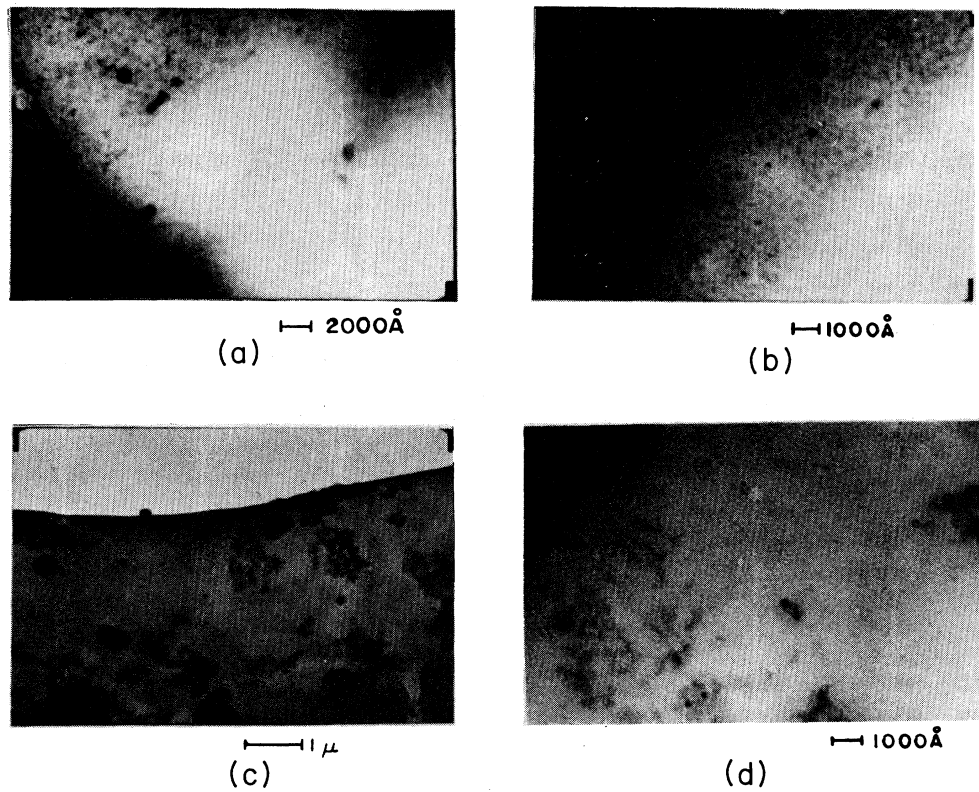


FIG. 2. Transmission electron micrographs of clustered and nonclustered Al-KCl composites: (a) $f=0.001$ Al ($a=399 \text{ \AA}$) sample; (b) $f=0.001$ Al ($a=103 \text{ \AA}$) sample; (c) $f=0.001$ clustered Al ($a=399 \text{ \AA}$) sample; (d) $f=0.001$ clustered Al ($a=103 \text{ \AA}$) sample.

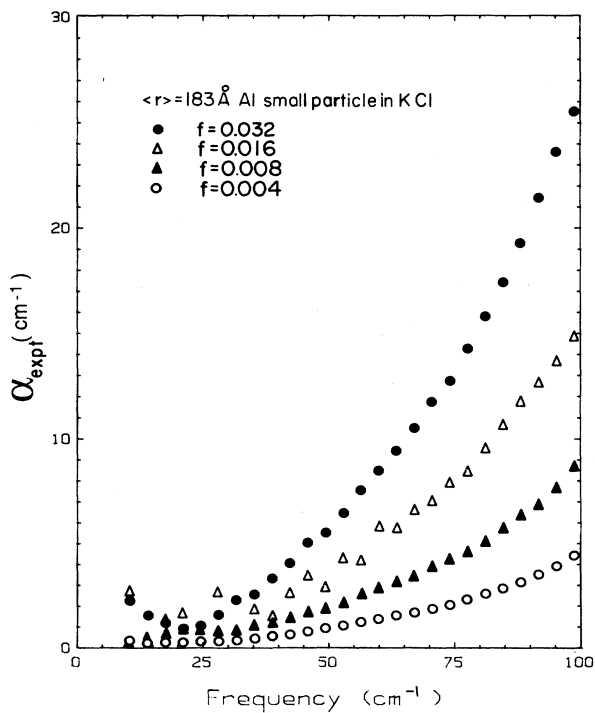


FIG. 3. FIR absorption coefficients of Al ($a=183 \text{ \AA}$) small-particle composites.

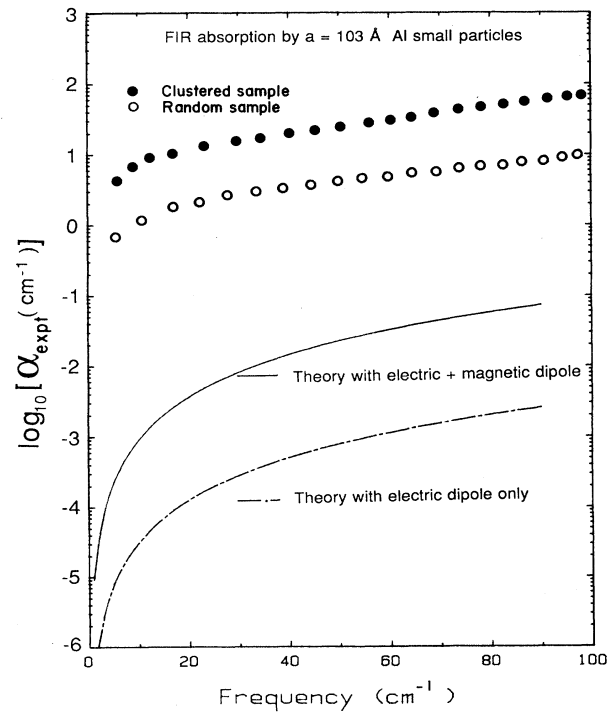


FIG. 4. FIR experimental results for $f=0.008$ clustered and nonclustered Al ($a=103 \text{ \AA}$) composites with the results of the classical calculation ($a=103 \text{ \AA}$, $f=0.008$).

are readily discerned in Figs. 2(a) and 2(b) whereas clusters of particles can be seen in Figs. 2(c) and 2(d).

Figure 3 shows representative FIR data, here for 183-Å average-radius aluminum-particle-KCl composites at four different volume fractions. The data can be shown to fit the following formula:

$$\alpha_{\text{expt}} = K_{\text{expt}} f \nu^2 + \alpha_0, \quad (2)$$

where K_{expt} is the proportionality constant in cm, ν is the frequency in cm^{-1} , and α_0 is the absorption of the dielectric medium. The proportionality constant K_{expt} can be a function of a number of variables, including

$$K_{\text{expt}} = K(\epsilon_m, \epsilon_i, a, f), \quad (3)$$

where ϵ_m (ϵ_i) is the dielectric constant of the metal (insulator), a is the radius of the particle, and f is the volume fraction. Notice that the volume-fraction dependence of the absorption coefficient is close to linear. In other words, K_{expt} is not a function of f , consistent with the results of previous FIR experiments for different metal particles. The nonlinear dependence in f in the earlier results⁵ could be due to the effect of interparticle tunneling within clusters of particles.

A comparison of the FIR absorption coefficients of clustered and nonclustered aluminum-particle-KCl composite samples is made in Fig. 4 for volume fraction $f=0.008$. The results of the classical calculation for isolated particles is shown. The curves are calculated from the electric dipole and magnetic dipole contribution to the absorption coefficient. According to the Maxwell-Garnett theory for very low frequency and in the low-volume-fraction limit,

$$\alpha = (K_e + K_m) f \nu^2 \quad (4)$$

with $K_e = 9\pi c \epsilon_i^{3/2} / \sigma_1$ and $K_m = 8\pi^3 a^2 \epsilon_i^{1/2} \sigma_1 / c$. Here, K_e and K_m are proportionality constants associated with the electric and magnetic dipole absorption, respectively, $c = 3 \times 10^{10}$ cm/sec, ϵ_i is the dielectric constant of KCl ($\epsilon_i = 4.84$), and σ_1 is the real part of the dc conductivity in esu units (sec^{-1}) with the electron relaxation time $\tau = a / v_F$ (v_F denotes Fermi velocity).

Both samples showed approximately the same frequency dependence but the magnitude of the absorption of the clustered one is about 7 times larger than that of the non-clustered sample. Also note that the measured FIR absorption coefficient for the nonclustered sample is still about 100 times larger than the theoretical prediction, consistent with the result of silver small particles in a gelatin matrix studied by Devaty and Sievers.⁶

The particle size dependence of the FIR absorption strength, K_{expt} , is shown in Fig. 5. Because the FIR absorption by the aluminum oxide coating is negligible,⁵ a correction to the experimental FIR absorption strength due to the oxide coating was made by taking into account the true volume fraction of the metal. The true volume fraction can be estimated as $f_{\text{correct}} = [a / (a - t)]^3 f$, where t is the thickness of the oxide shell on the particle. Then

$$K_{\text{correct}} = [a / (a - t)]^3 K_{\text{expt}} \quad (5)$$

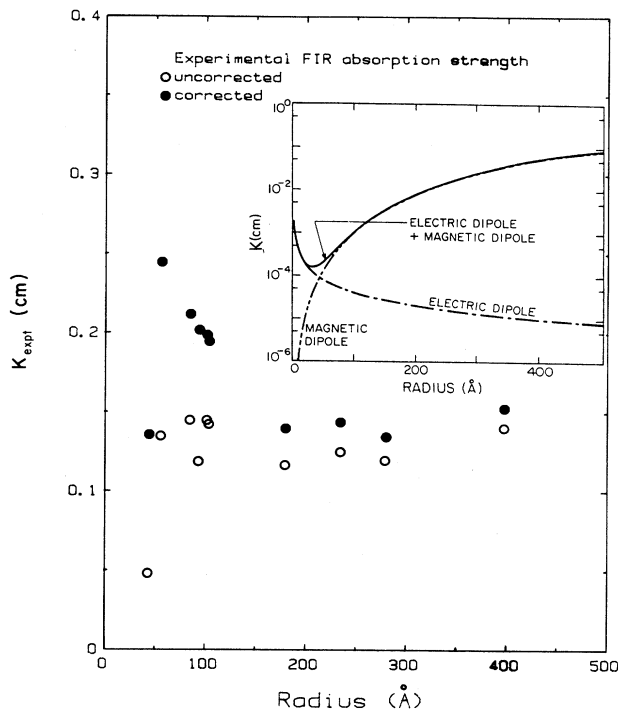


FIG. 5. K_{expt} (open circle) and K_{correct} (solid circle) vs particle size.

because we overestimated the metallic volume fraction. Here, a is the overall particle radius measured through the STEM analysis and t is the thickness of the oxide coating estimated by comparing the dark-field STEM picture with the corresponding bright-field picture. The corrected results are shown as the solid circles in Fig. 5. Theoretical results are shown in the small inset. The curves in the inset are calculated by assuming (as is usually done) that the mean free path of the electrons in the metal particle equals the particle radius. The disagreement of the measured K_{expt} with K_{theory} is not only in the magnitude of absorption but also in its functional form.²⁵ However, the oxide coating-corrected data points follow the electric dipole absorption curve even though the mag-

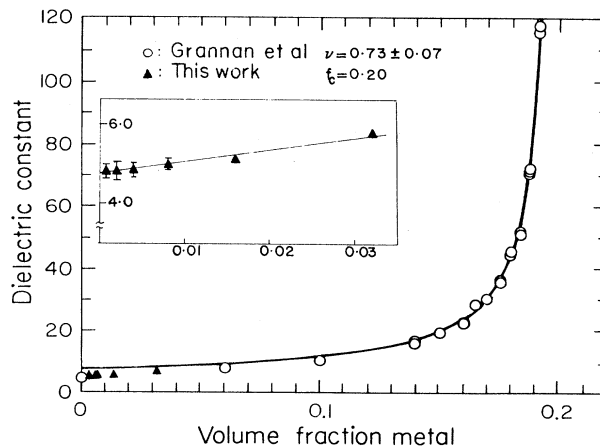


FIG. 6. Dielectric constants of Al-KCl composites.

nitude of the experimental data points is substantially larger than that of the calculation. Such a remarkable discrepancy suggests that the intrinsic electrical properties of a small particle could be different from what we have believed to be correct (e.g., the concept of small "Drude metal" particle and the surface scattering approximation, etc.).

The FIR dielectric constant, obtained from the Fourier analyses of the interference fringes, is shown in Fig. 6. The enhancement in the FIR dielectric constant of the composites with increasing metal volume fraction agrees with the audio frequency results of Grannan *et al.*²⁶

IV. CONCLUSION

We have demonstrated that the anomalous FIR absorption by small particles is still observed in samples in which direct STEM analyses do not show clustering of particles. The measured absorption coefficients are still about 2 orders of magnitude larger than the classical calculation for order of 100-Å aluminum particles, too large to be interpreted as the FIR tail of the resonance due to the surface plasmon predicted by the classical theory.

Also, the particle size dependence study suggests that

whatever the FIR absorption mechanisms are, the anomalous FIR behavior of the small particles does not arise from the small "Drude metal particle." However, as the size of the particle gets larger, we anticipate that the small particle will recover its bulk metallic properties and the FIR absorption strength K_{expt} will converge to the classical value, dominated by the magnetic dipole absorption, which increases quadratically in particle radius [see Eq. (4)]. In fact, this tendency has been observed by Lee *et al.*⁷ for fairly large silver particles ($a > 500$ Å).

Therefore, by referring to all the evidence we have, we conclude that the Drude description of a small particle may not be adequate to explain the anomalous small-particle properties in the FIR and that further systematic study is necessary to have more detailed information about the nature of the dielectric function of a small particle.

ACKNOWLEDGMENT

We would like to thank Dr. J. Newkirk at the Major Analytical Instrument Center (MAIC) of the University of Florida for help with the STEM analyses.

*Present address: Department of Physics, ML 11, University of Cincinnati, Cincinnati, OH 45221.

¹For a review, see G. L. Carr, S. Perkowitz, and D. B. Tanner, *Far Infrared Properties of Inhomogeneous Materials*, Vol. 15 of *Infrared and Millimeter Waves*, edited by K. J. Button (Academic, Orlando, 1984).

²D. B. Tanner, A. J. Sievers, and R. A. Buhrman, *Phys. Rev. B* **11**, 1330 (1974).

³C. G. Granqvist, R. A. Buhrman, and A. J. Sievers, *Phys. Rev. Lett.* **10**, 625 (1976).

⁴N. E. Russe, J. C. Garland, and D. B. Tanner, *Phys. Rev. B* **23**, 632 (1981).

⁵G. L. Carr, R. L. Henry, N. E. Russell, J. C. Garland, and D. B. Tanner, *Phys. Rev. B* **24**, 777 (1981).

⁶R. P. Devaty and A. J. Sievers, *Phys. Rev. Lett.* **52**, 1344 (1984).

⁷S. I. Lee, T. W. Noh, K. Cummings, and J. R. Gaines, *Phys. Rev. Lett.* **55**, 1626 (1985).

⁸T. W. Noh, S. I. Lee, Y. Song, and J. R. Gaines, *Phys. Rev. B* **34**, 2882 (1986).

⁹The actual linewidth of the surface plasmon peak is broader than the predictions given by the classical theory by a factor of 2 or more.

¹⁰L. P. Gor'kov and G. M. Eliashberg, *Zh. Eksp. Teor. Fiz.* **48**, 1407 (1965) [*Sov. Phys.—JETP* **21**, 940 (1965)]. Also, see S. Strassler, M. J. Rice, and P. Wyder, *Phys. Rev. B* **6**, 2575 (1972); R. P. Devaty and A. J. Sievers, *ibid.* **21**, 2123 (1980).

¹¹A. A. Lushnikov and A. J. Simonov, *Phys. Lett.* **44A**, 45 (1973).

¹²D. M. Wood and N. W. Ashcroft, *Phys. Rev. B* **25**, 6255 (1982).

¹³A. J. Glick and E. D. Yorke, *Phys. Rev. B* **18**, 2490 (1978).

¹⁴H. J. Trodahl, *J. Phys. C* **15**, 7245 (1982); A. G. Mal'shukov, *Solid State Commun.* **44**, 1257 (1982).

¹⁵E. Simanek, *Phys. Rev. Lett.* **38**, 1161 (1977).

¹⁶P. N. Sen and D. B. Tanner, *Phys. Rev. B* **26**, 3582 (1982).

¹⁷W. A. Curtin and N. E. Ashcroft, *Phys. Rev. B* **31**, 3287 (1985).

¹⁸P. M. Hui and D. Stroud, *Phys. Rev. B* **33**, 2163 (1986).

¹⁹F. Claro and R. Fuchs, *Phys. Rev. B* **33**, 7956 (1986).

²⁰G. A. Nickasson, S. Yatsuya, and C. G. Granqvist, *Solid State Commun.* **59**, 579 (1986).

²¹C. G. Granqvist and R. A. Buhrman, *J. Appl. Phys.* **47**, 2200 (1976).

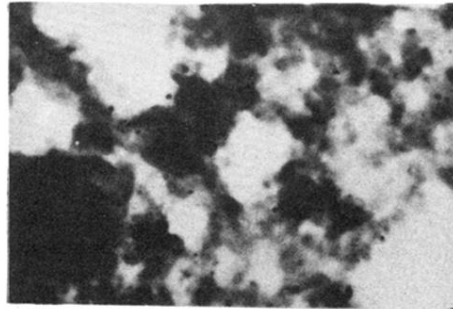
²²R. L. Henry and D. B. Tanner, *Infrared Phys.* **19**, 163 (1979).

²³R. B. Sanderson and H. E. Scott, *Appl. Opt.* **10**, 1097 (1971).

²⁴G. L. Carr, Ph.D. thesis, The Ohio State University, 1982.

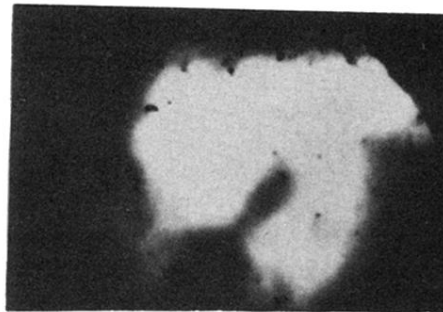
²⁵The effect of including particle size distribution would tend to flatten out the K versus radius curve. The flattening is aided by the fact that for size distributions which have a significant volume fraction of rather large particles, the skin depth becomes important at far-infrared frequencies.

²⁶D. M. Grannan, J. C. Garland, and D. B. Tanner, *Phys. Rev. Lett.* **46**, 375 (1981).



10000Å

(a)



10000Å

(b)

FIG. 1. Transmission electron micrographs of Al-KCl composites: (a) chemically polished $f=0.032$ Al ($a=85 \text{ \AA}$) sample (reground six times); (b) ion milled $f=0.001$ Al ($a=399 \text{ \AA}$) sample (reground four times).

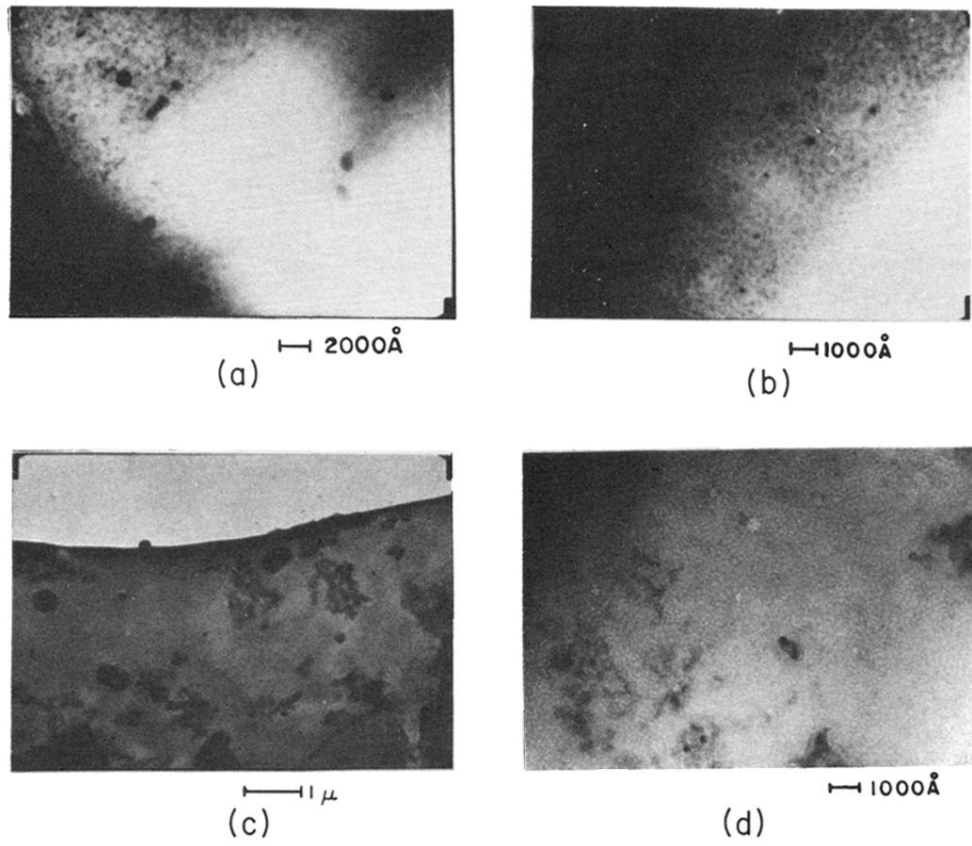


FIG. 2. Transmission electron micrographs of clustered and nonclustered Al-KCl composites: (a) $f=0.001$ Al ($a=399\ \text{\AA}$) sample; (b) $f=0.001$ Al ($a=103\ \text{\AA}$) sample; (c) $f=0.001$ clustered Al ($a=399\ \text{\AA}$) sample; (d) $f=0.001$ clustered Al ($a=103\ \text{\AA}$) sample.